Spatiotemporal Variations in the Completeness Magnitude of the Composite Alberta Seismicity Catalog (CASC)

by Luqi Cui and Gail M. Atkinson

ABSTRACT

We employ a network-based method to map the spatiotemporal variations of the magnitude of completeness (M_c) in the Composite Alberta Seismicity Catalog (CASC; see Data and Resources) from 1985 to 2015 across a grid of sites. The underlying principle is that we expect events to be located and cataloged if they are detected on four or more seismic stations. Seven M_c maps are created to represent spatial variations of M_c in time periods: 1985–1989, 1990–1999, 2000–2006, 2007–2009, 2010, 2011–2013, and 2014–2015. By counting the annual number of events above M_c since 1985, and assuming a Gutenberg–Richter *b*-value of 1.0, we calculate the equivalent number of $\mathbf{M} \geq 3$ earthquakes in eight relatively active grid cells. In several areas, there is clear evidence of changes of seismic rate over time. Overall, seismicity in Alberta is highly clustered in both space and time.

INTRODUCTION

Alberta is an area of relatively low seismic activity (Milne, 1970; Milne *et al.*, 1978; Stern *et al.*, 2013; Schultz, Stern, Gu, *et al.*, 2015), but there has been growing concern over increasing seismicity levels due to oil and gas activities including hydraulic fracturing operations (BC Oil and Gas Commission, 2012; Atkinson *et al.*, 2015; Eaton and Mahani, 2015; Farahbod *et al.*, 2015; Schultz, Stern, Novakovic, *et al.*, 2015), wastewater disposal (Horner *et al.*, 1994; Schultz *et al.*, 2014), and gas extraction (Baranova *et al.*, 1999). Over the last decade, there has been significant growth in the seismographic network density (e.g., Stern *et al.*, 2013; Fereidoni and Cui, 2015), making it difficult to distinguish between rate increases due to oil and gas extraction and rate increases due to improving detection levels. There has also been a proliferation of agencies reporting seismicity (including the Geological Survey of Canada, the Alberta Geological Survey, the U.S. Geological Survey, and Nanometrics Inc.). Fereidoni and Cui (2015) compiled all of the contributed public catalogs into a Composite Alberta Seismicity Catalog (CASC) that is available online (see Data and Resources). This catalog contains all available information on events from these sources, including the alternative estimates of magnitudes and locations. An important aspect of the CASC is that the magnitude of completeness varies greatly in time and space. In this article, we aim to estimate the completeness of the information in the CASC regionally, and map its variability in time and space. This is a challenging exercise because the levels of seismicity are too low in most parts of the study area to enable statistical methods to be employed. Moreover, the rates of seismicity may be changing in time due to anthropogenic activities. The approach taken here is also applicable to other similar regions (such as the central United States) for which we may need to understand the spatiotemporal variation of the magnitude of completeness.

The detection capability of a seismic network depends on many factors, including the station density, the geographic distribution of stations, site conditions, recording characteristics, and signal-processing methods (Schorlemmer and Woessner, 2008). The magnitude of completeness (M_c) is an oft-cited measure of this capability. M_c is defined as the lowest magnitude for a specific spatial area during a specific time period, for which 100% of the earthquakes that occurred are detected (Rydelek and Sacks, 1989). In general, the development of seismic networks significantly improves the detection threshold M_c; however, this also means that M_c changes in time and space as new seismic stations are added, complicating its determination. An accurate assessment of M_c is important because underestimation or overestimation of M_c in statistical analysis may lead to biased estimates of Gutenberg–Richter parameters, and/or to overtrimming of catalog data. In particular, a reliable estimation of M_c is required to assess seismicity rate changes, compute magnitude recurrence parameters, and for purposes of earthquake forecasting (Mignan *et al.*, 2011; Mignan and Woessner, 2012). It is because of the importance of M_c that a number of techniques to evaluate or map M_c have been developed.

Mignan and Woessner (2012) provide a comprehensive overview of approaches to M_c estimation, which can in general be classed as catalog-based methods and network-based methods. The catalog-based methods are mostly based on the assumption of self-similarity of the earthquake process (Wiemer and Wyss, 2000; Woessner and Wiemer, 2005; Mignan *et al.*, 2011); specifically, M_c is taken as the minimum magnitude at which the observed cumulative frequency–magnitude distribution departs from the Gutenberg–Richter (G-R) relation

doi: 10.1785/0220150268

(Gutenberg and Richter, 1944). Network-based methods use the network distribution to estimate M_c based on the proximity to seismic stations (Schorlemmer *et al.*, 2010; Mignan *et al.*, 2011; Plenkers *et al.*, 2011). Here we focus on a network-based approach because it is most suitable given the data constraints in this region.

METHODOLOGY FOR ESTIMATING AND MAPPING M_c

In this study, we employ a network-based method to map the spatiotemporal variations of M_c in Alberta and its surrounding area. This method is applied to compute the completeness of the CASC catalog from 1985 to 2015 across a grid of sites covering the study area. The underlying principle is that events should be located and cataloged if they are detected on four or more seismic stations that are operational at the time. Thus, we can use the locations and magnitudes of events in the catalog, in combination with the station distribution, to infer the required conditions for detectability, and map their variations in time and space. We model the function $M_c\ (x_i, y_i, \Delta t)$:

$$M_c(x_i, y_i, \Delta t) = c_1 D_4(\Delta t) + c_2, \qquad (1)$$

in which $M_c\ (x_i, y_i, \Delta t)$ is the minimum magnitude that can be detected at a node point located in the center of a cell on the grid (at longitude x_i, latitude y_i) in time period Δt, and D_4 (Δt) is the distance from the epicenter of an earthquake to its fourth nearest recording station in the same time period (arc length between the coordinates). c_2 is the distance within which we would require four stations to locate an event of $M = 0$, whereas c_1 denotes the increase in D_4 per magnitude unit. We determine the coefficients c_1 and c_2 using the CASC catalog (Fereidoni and Cui, 2015) and a list of stations (including on–off dates) to find what events have been reported in the catalog, at what station distances. (Note: we know the operational start and stop dates for each station, and make the assumption that they were operating continuously during this time, ignoring any occasional outages that may have occurred, because we do not have this level of detailed information.) We choose the fourth nearest station because network practice in Alberta has been to locate and catalog earthquakes if they were detected on four or more stations. When considered *a priori*, the estimate of M_c based on station distribution can be updated in areas where there are sufficient events to make a statistical estimate (about 200; see Mignan *et al.*, 2011). An advantage of the approach is that once the conditions for detectability have been defined in the region, one can map M_c and its uncertainties in both time and space over a grid of sites, including grid points where the seismicity rate may be too low to examine statistically.

Figure 1 provides an overview of the station coverage and $M > 1.5$ events in different time periods considered in this study. The time periods of 1985–1989 and 1990–1999 are merged into one map (Fig. 1a) because they had only minor changes of stations. When modeling the relation between M_c and D_4, all events reported above zero magnitude are plotted (Fig. 2). The stations and their operational dates are summarized from Natural Resources Canada (NRcan, 2015; see Data and Resources), Stern *et al.* (2013), and Nanometrics Inc. in Table 1. We compute D_4 (Δt) for every event in the catalog and plot it against magnitude to draw conclusions regarding M_c. We recognize that some temporary stations (such as those deployed for aftershock studies) may not appear in our regional lists and may have increased the magnitude of completeness relative to that mapped here for short periods of time in specific regions. The Rocky Mountain House (RMH) region is a good example of this, as it has been active for decades and hosted several temporary networks that have contributed events to the literature.

RESULTS

M_c Function

To derive a function $M_c = f(D_4)$, we need to consider a catalog dataset for which the underlying seismic network distribution experienced a minimal number of changes; this allows a robust relationship between station locations and catalog events to be defined. For this purpose, we focus on the events contained in the CASC from August 2013 to January 2015, as located by Nanometrics Inc. (NMX catalog; Fereidoni and Cui, 2015) using a consistent number of stations (Fig. 1f). Figure 2 shows the computed distance to the fourth nearest station (D_4) for these events, considering their moment magnitudes (**M**) and local magnitudes (M_L) (see Data and Resources, and Fereidoni and Cui, 2015, for information on magnitude determinations and conversions for the CASC); the locations of the events in space are also illustrated. We note that events are spread along the Alberta–British Columbia border region, and occur during both daytime and nightime hours (thus representing both high- and low-background noise conditions). Events with $\mathbf{M} < 2$ are reported as M_L, and have generally been recorded in areas where a number of stations are concentrated, with $D_4 < 25$ km. Larger events ($\mathbf{M} > 2$) spread from small D_4 (~30 km) to large D_4 (~300 km) as magnitude increases. From **M** 2.0 to 3.6, there is an obvious trend if we link all the largest values of D_4 together; this trend delineates the smallest magnitude that can be located for a given value of D_4. If events are smaller than this, the stations are too distant to provide the required four-station detection.

To better describe the D_4 versus **M** variation, Figure 3 provides a percentile plot to show the distribution of values of D_4; values of **M** (Fig. 2b) are rounded to one decimal to enable binning. The lower, inner, and upper lines of the boxes are the 25%, 50%, and 75% quartiles of the typical distance distribution for the fourth closest station at each magnitude level. It is important to recognize that the points near the upper range of the distribution are not outliers. Rather, these points are highly significant as they characterize the farthest distance that an earthquake in each magnitude level can be detected by at least four seismic stations—though we recognize that in some cases this may also represent ideal observational conditions, such as low noise. The upper ranges of the plotted points form a straight line:

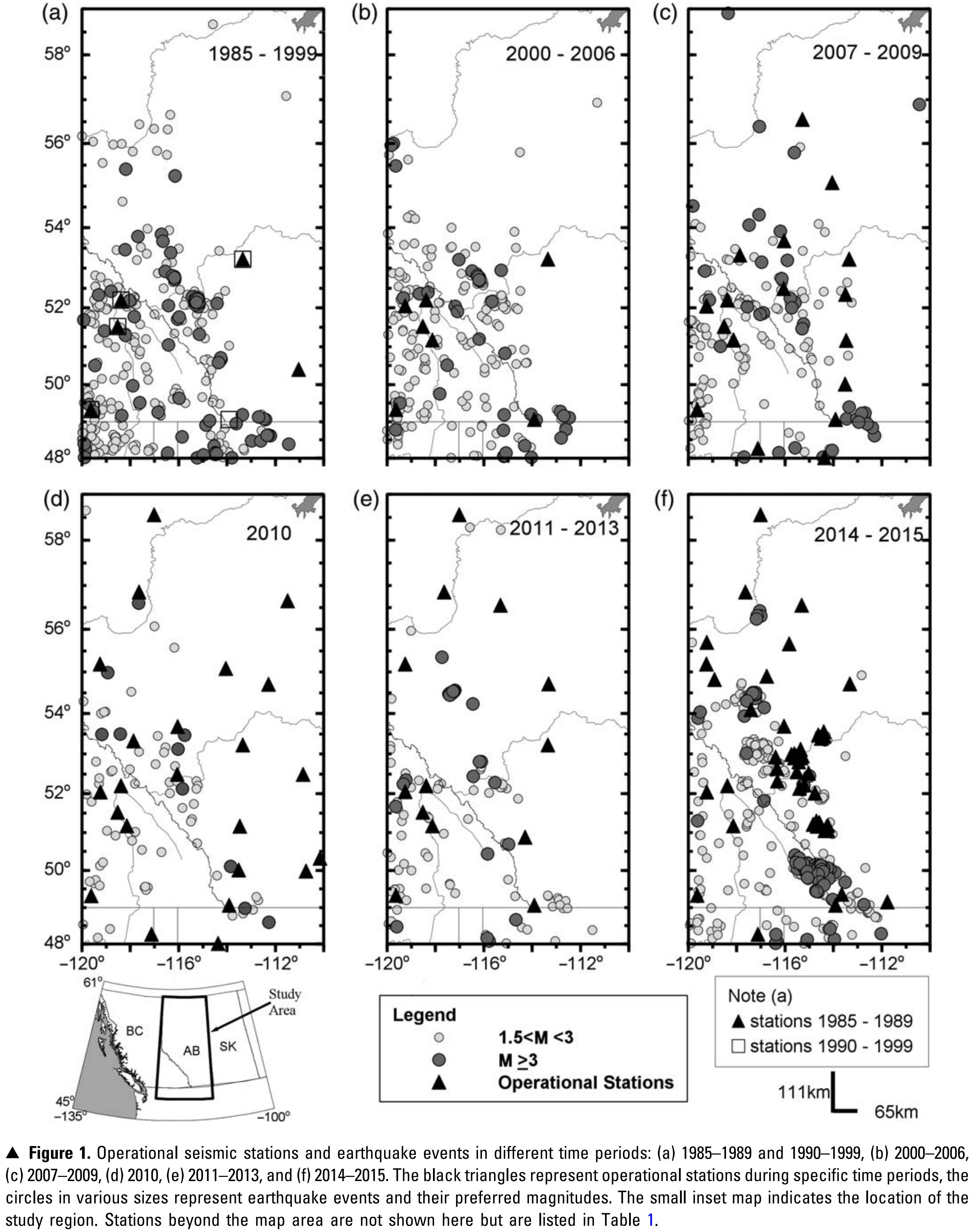

▲ **Figure 1.** Operational seismic stations and earthquake events in different time periods: (a) 1985–1989 and 1990–1999, (b) 2000–2006, (c) 2007–2009, (d) 2010, (e) 2011–2013, and (f) 2014–2015. The black triangles represent operational stations during specific time periods, the circles in various sizes represent earthquake events and their preferred magnitudes. The small inset map indicates the location of the study region. Stations beyond the map area are not shown here but are listed in Table 1.

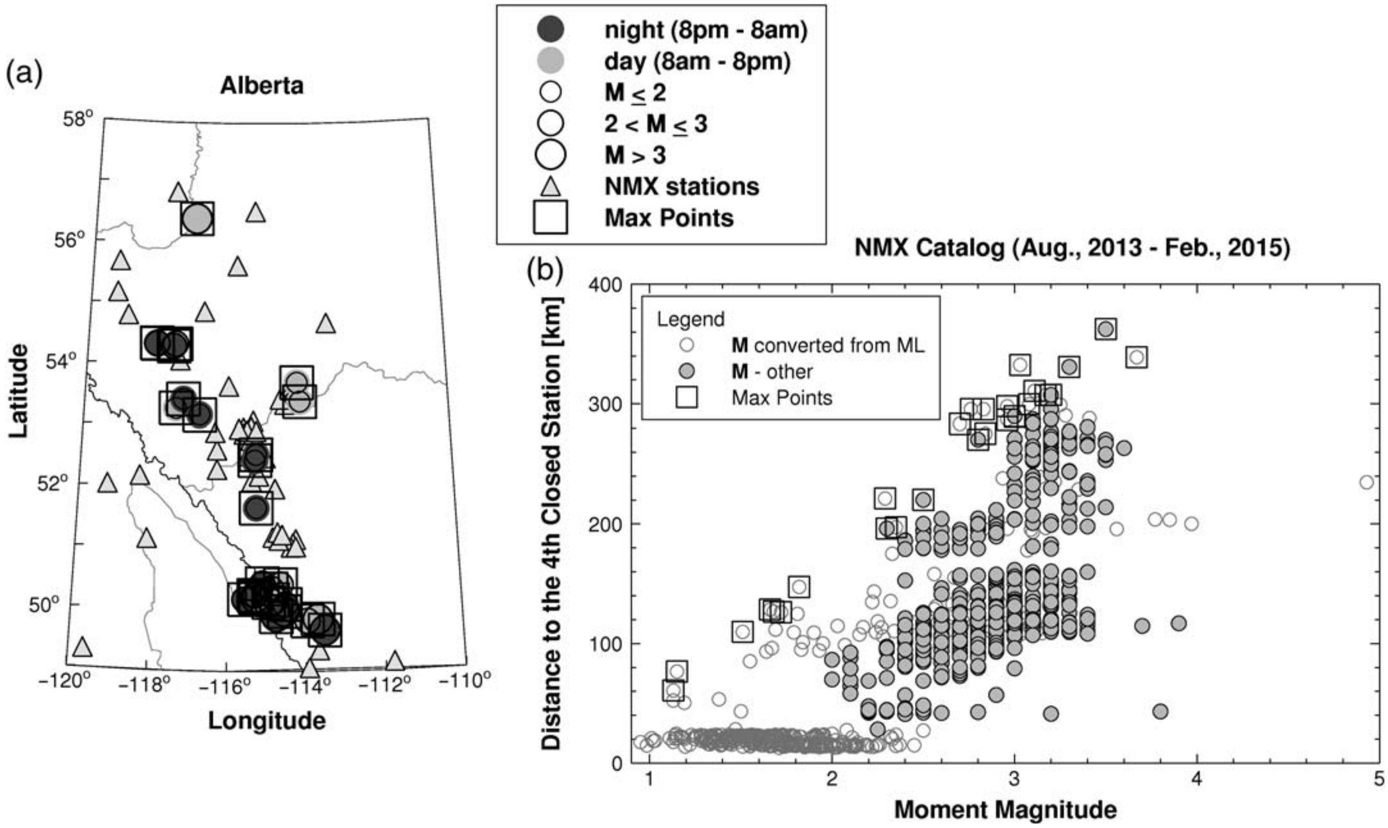

▲ **Figure 2.** Earthquakes in NMX catalog (August 2013–January 2015) used to derive function $M_c = f(D_4)$. (a) Map of spatiotemporal distribution of events (squares show events having maximum D_4, as highlighted in b). (b) Distance to the fourth nearest station (D_4) versus **M** for events in NMX catalog, with maximum D_4 values boxed by squares; where an estimate of **M** was not directly available, conversion was made using $\mathbf{M} = M_L + 0.12$.

$$D_4 = 132.16M_c - 82.398. \quad (2)$$

The lack of points along this line for intermediate magnitudes may simply indicate a lack of applicable observations in this brief time window (August 2013 to January 2015), which would be filled in over a longer time period. We therefore base equation (2) on the upper-bounding points, as marked by boxes in Figure 3.

We rearrange equation (2) to express the minimum magnitude of events that can be detected by at least four stations located at a maximum distance of D_4 from the earthquake:

$$M_c(x_i, y_i, \Delta t) = [D_4(\Delta t) + 82.398]/132.16, \quad (3)$$

with (x_i, y_i) indicating the longitude and latitude of grid cells, for each of which we calculate D_4 based on the station configuration at time period Δt.

Spatiotemporal Evaluation of M_c in the CASC

We subdivide the CASC into several time periods during which the network configuration was relatively stable (i.e., few changes in stations in Fig. 1). Until about a decade ago, all of the stations were national network stations operated by the Geological Survey of Canada, with stations being gradually added in time (there were only eight stations in 1985, increasing to 21 stations in 2013) (see Data and Resources). The Alberta Geological Survey (AGS) and universities in Alberta added stations over the years from 2006- 2010 (Stern *et al.*, 2013), then the TransAlta/Nanometrics network added multiple stations in 2013-2014 (see Data and Resources). By looking at the distribution of station additions over time, we decided on the following time periods (inclusive): 1985–1989, 1990–1999, 2000–2006, 2007–2009, 2010, 2011–2013, and 2014–2015. We consider the stations that have been operating since the beginning of each time period (and that are generally operational for the entire period) when calculating the M_c values.

We represent the study area by a uniform spatial grid with 55 by 55 nodes spaced at 0.2° latitude and 0.2° longitude (22 km by 13 km). The value of D_4 at each node is calculated from the station configuration for the applicable time period. Equation (3) is then used to compute M_c values for all nodes. Our method works well in areas of good coverage but is poorly constrained for areas lacking stations, and as the edges of the map are approached. Hence we need to impose an upper bound on M_c. According to Adams and Halchuk (2003), M_c should not exceed 3.5 in the area of interest in the timeframe of our study, and we therefore impose a maximum value of $M_c = 3.5$. By constraining the maximum value of M_c to 3.5, the largest

Table 1 Operational Time of Each Seismic Station for the Composite Alberta Seismicity Catalog (CASC)			
Time Period	Number of Stations	Added Stations	Shut Down Stations
1985–1989	8	EDM, DOWB, FSB, MNB, PNT, FCC, ULM, and SES (NRcan, 2015)	
1990–1999	9	YKW3 and WALA (NRcan, 2015)	SES
2000–2006	14	SLEB, LLLB, FNBB, BMBC, and BLBC (NRcan, 2015)	
2007–2009 (AGS)	36	YKR1, YKR2, YKR4, YKR9, DGMT, EGMT, NEW, YKB3, YKB6, BSMT, JTMT, OVMT, SWMT, YBMT, BLMT, NOR, PER, BRU, CLA, LYA, HON, and DOR (Stern *et al.*, 2013)	
2010 (AGS)	43	CZA, FMC, HLO, MHB, MEDA, WAPA, MANA, and HILA (Stern *et al.*, 2013)	DOR
2011–2013	19 (continuous with time 2000–2006)*	HILA, MANA, PRDA, WAPA, and UBRB (NRcan, 2015)	
2014–2015	54	TransAlta/Nanometrics stations and some national stations (TD 001–TD013, TD022–TD029, TD016, TD06A, TD07A, TD08A, TD09A, TD13A, TD.CRF, US. EGMT, US.NEW, LGPLA, TD.COP01, Y5.PER, BDMTA, BRLDA, HSPGA, MKRVA, STPRA, SWHSA, WTMTA, ATHA, HILA, RDEA, MANA, WAPA, CN. LLLB, CN.PNT, CN.WALA, CN.MNB, CN.BLBC, CN. SLEB, CN.NBC4, CN.NBC5, and CN.NBC6) (NRcan, 2015) (see Data and Resources)	

*There are 43 operational stations used by the Alberta Geological Survey (AGS) (Stern *et al.*, 2013) in this time period, but there is no real-time cataloging of events; the AGS catalog using these stations is at present complete only to 2010.

distance D_4 should be not greater than 380 km (equation 2). Moreover, because D_4 must be greater than zero, M_c should not be smaller than 0.62 (equation 3). In our study, D_4 is always greater than 10 km, even for the densest distribution of stations that we have since 2014. Thus, our estimation of M_c should be greater than 0.7. The range of distance D_4 is therefore limited to the range [10 km, 380 km]. Figure 4 maps the spatiotemporal variations of M_c in six contour maps for different time periods: 1985–1989, 1990–1999, 2000–2006, 2007–2009, 2010, and 2011–2013. Figure 5 provides equivalent information for the most recent and complete time period, from mid-2014 to 2015. As the number of seismograph stations increases, smaller M_c values are estimated, especially for the 2007–2010 time period with the addition of AGS network stations, and since mid-2014 to 2015 with the addition of the TransAlta/Nanometrics array.

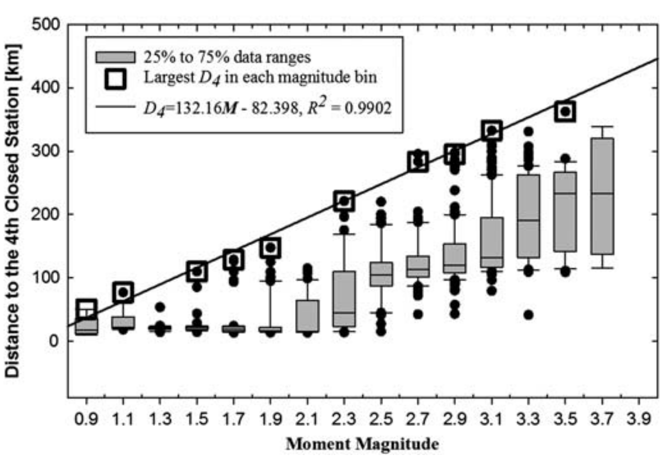

▲ **Figure 3.** Percentile plot for 2013–2015 NMX catalog. The circles represent earthquake events. The lower, inner, and upper lines of the boxes represent the 25%, 50%, and 75% quartiles, respectively, for D_4 for all events in each magnitude bin.

For the central region of the study area, we note in Figures 4 and 5 that the minimum value of M_c in the most recent catalogs, from 2007 to the present, is < 1.0, which is significantly smaller than the minimum M_c ($2.0 \sim 3.5$) available in the earthquake catalog that is provided as a standard online product of the Geological Survey of Canada (GSC); this is because the GSC catalog does not use all of the stations. Investigating the temporal behavior of M_c for both the AGS and GSC catalogs is useful because the CASC uses both of these sources, and thus the lower of the two M_c values will govern. The recent addition of the TransAlta/Nanometrics stations strongly enhances the detection capability in western Alberta.

DISCUSSION

Comparison of Results with Other Studies

Statistical seismology relies on robust and comprehensive knowledge of the magnitude of completeness of earthquake catalogs

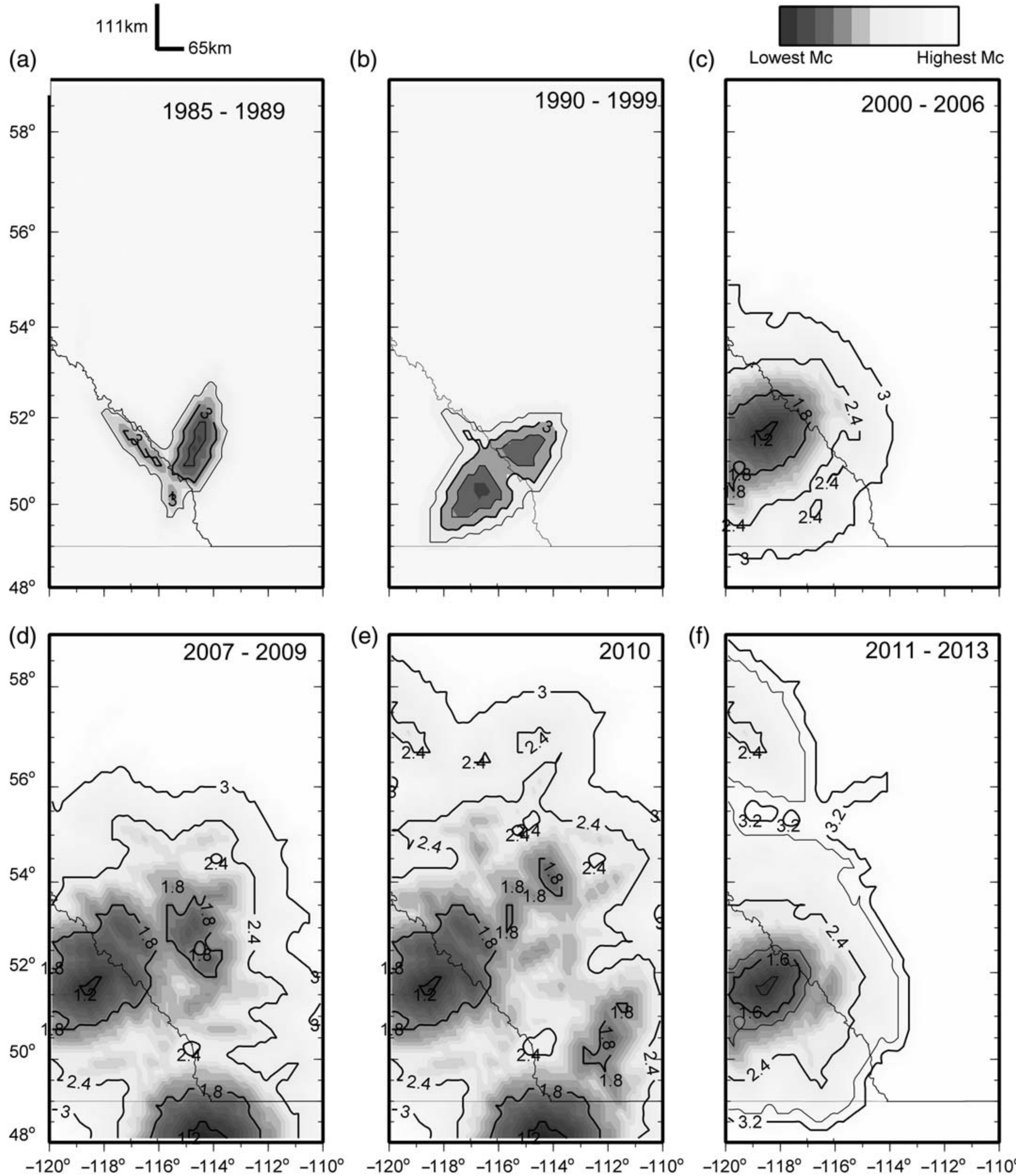

▲ **Figure 4.** Contour maps of estimated M_c for the Composite Alberta Seismicity Catalog (CASC): (a) 1985–1989; (b) 1990–1999; (c) 2000–2006; (d) 2007–2009; (e) 2010; and (f) 2011–2013.

and their variability in time and space. This is particularly important for the study of induced seismicity, as we need to be able to distinguish real rate changes from those that may be a consequence of improving station coverage. The method used in this study is advantageous because it is suitable for use with a sparse catalog and a station distribution that changes frequently

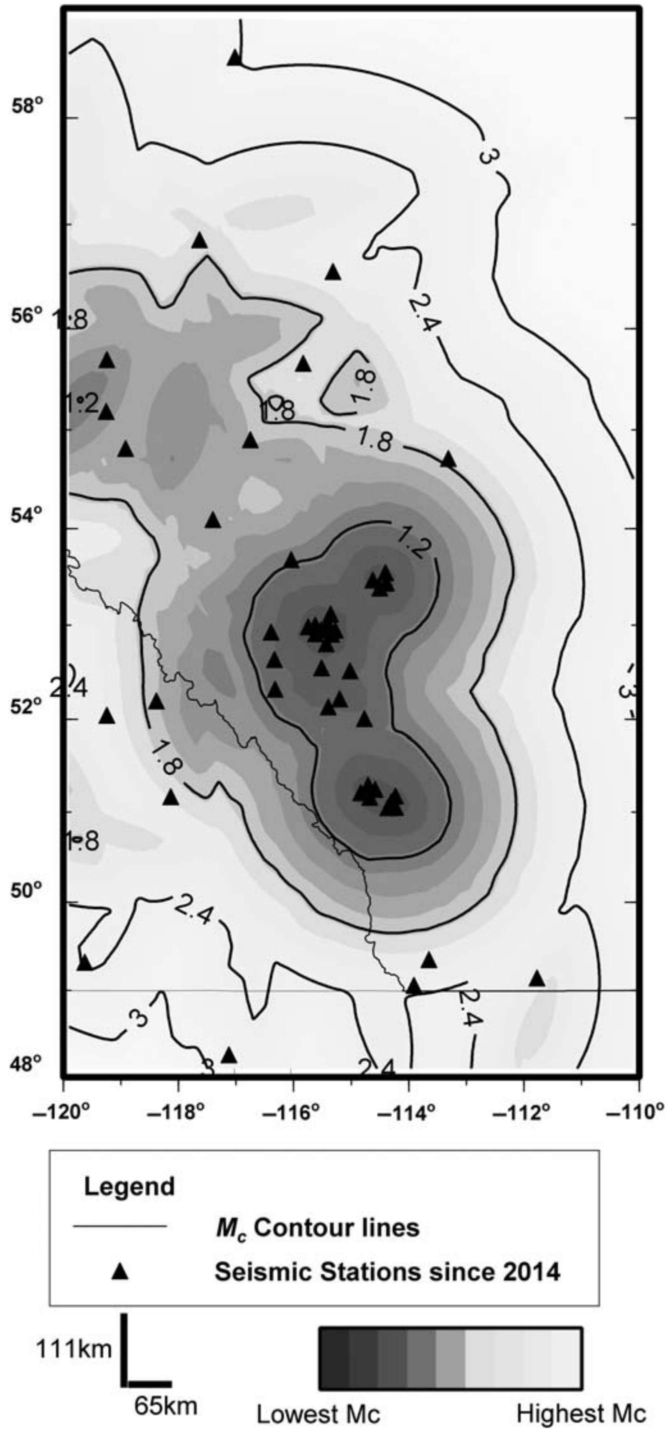

▲ **Figure 5.** Estimated M_c for the CASC for the time period mid-2014 to 2015. The black triangles represent the operating seismic stations.

over time, for which statistical methods are not applicable; the method also enables the mapping of M_c in a systematic way in both time and space.

Our method is based on a linear relationship between M_c and D_4 that is derived from the station distribution and catalog observations (Figs. 2 and 3). Such a relationship has been ex-

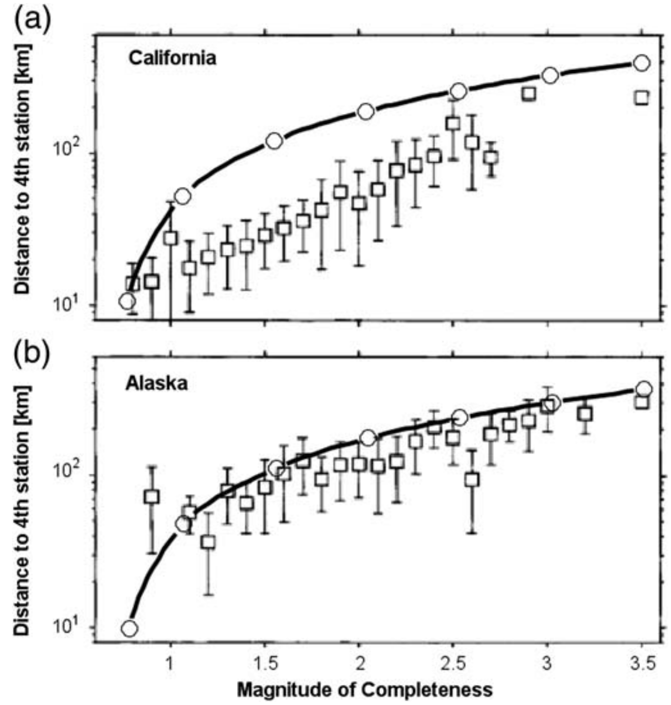

▲ **Figure 6.** Distance to the fourth nearest station as a function of M_c for (a) California and (b) Alaska (modified from Wiemer and Wyss, 2000), compared to the estimation of M_c for the Alberta area from this study, for 2013–2014 (curved lines with circle markers).

hibited in previous studies (Wiemer and Wyss, 2000; Mignan *et al.*, 2011; Schultz, Stern, Gu, *et al.*, 2015) in slightly different forms. For example, for a California catalog and an Alaska catalog, Wiemer and Wyss (2000) determined the magnitude of completeness from a study of the statistics of events (Gutenberg–Richter *b*-values across a grid of sites, using 250 events for each *b*-value). They showed that their determined M_c values are closely correlated with the distance to the fourth-closest station. In Figure 6, we compare our estimate of M_c based on D_4 with their observations of fitted M_c versus D_4. Wiemer and Wyss use a linear relationship between $\log_{10} D_4$ and M_c, whereas our observations suggested that a simple linear relation between D_4 and M_c was adequate. Our relation is very similar to the Wiemer and Wyss relation for Alaska but not for California. In California, the corresponding M_c is significantly lower for a given value of D_4. We speculate that Alberta and Alaska have more favorable noise conditions on average, due to their relative remoteness from population centers; it is also possible that attenuation is more pronounced in California, reducing the distances to which the signals can be detected.

In our study, there are no areas with sufficient seismicity to allow meaningful Bayesian updating of M_c based on further statistical analyses, as was performed by Mignan *et al.* (2011). Similarly, departures from a Gutenberg–Richter relation as employed by Wiemer and Wyss (2000) are not feasible with the sparse seismicity. Moreover, we do not wish to assume stationarity of seismicity or a Gutenberg–Richter relation *a priori*. Therefore, we have concentrated on use of the catalog to define

M_c, assuming that M_c will increase steadily with D_4. This was the rationale for drawing a linear relationship between D_4 and M_c, though an alternative logarithmic form could also be used, and would provide similar results in the magnitude range of interest (e.g., at $\mathbf{M} \geq 2$).

The results of our method for Alberta may be compared with the results of Schultz, Stern, Gu, *et al.* (2015). Schultz, Stern, Gu, *et al.* (2015) investigated M_c by combining an analysis of noise levels in waveform data with the simulation of earthquake spectra to quantify station and network performance. They define M_c as the minimum magnitude that should allow for detection and picking of four P phases, which they compute on a grid approximately 5×5 km^2 (for a fixed focal depth of 5 km). The M_c of Schultz, Stern, Gu, *et al.* (2015) should be more precise in picking the first four detectable stations and estimating D_4. However, their method is theoretical rather than empirical, and thus the calculated M_c may not always be realized in practice. Moreover, they do not address changes in M_c over time; their study applies to the station distribution used by the AGS as of 2010. We compare our results with those of Schultz, Stern, Gu, *et al.* (2015) for 2010 in Figure 7. The results are consistent, with both studies suggesting that M_c is close to 2.0 in southern Alberta and increases to 3.0 or above in the north.

Preliminary Statistical Analysis of Seismicity Rates

With completeness thresholds determined since 1985, and magnitudes converted uniformly to moment magnitude **M** in the CASC, average seismicity rates and their variability can now be examined. For this exercise, we use a grid of cells that are 0.5° in latitude and 1° in longitude, as shown in Figure 8.

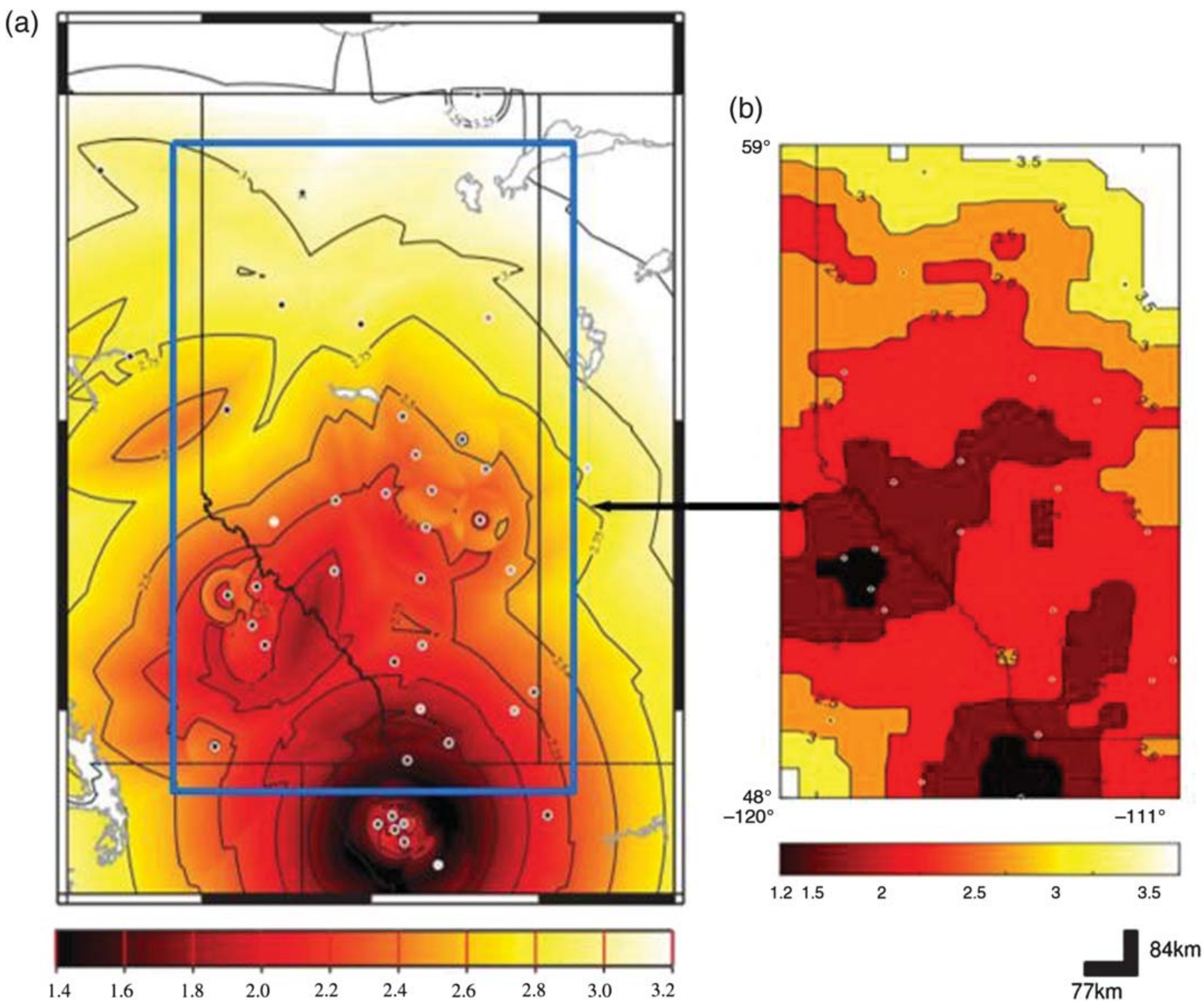

▲ **Figure 7.** Comparison of the estimated magnitude of completeness (M_c) in 2010. (a) reprinted from Schultz, Stern, Gu, *et al.* (2015) and (b) based on our method. The colored contours indicate spatial variations of M_c. The circles depict seismic stations used for computing M_c in (a), whereas the blue rectangle shows our study area (with its M_c plotted at b); our study area is smaller than the Schultz mapping area.

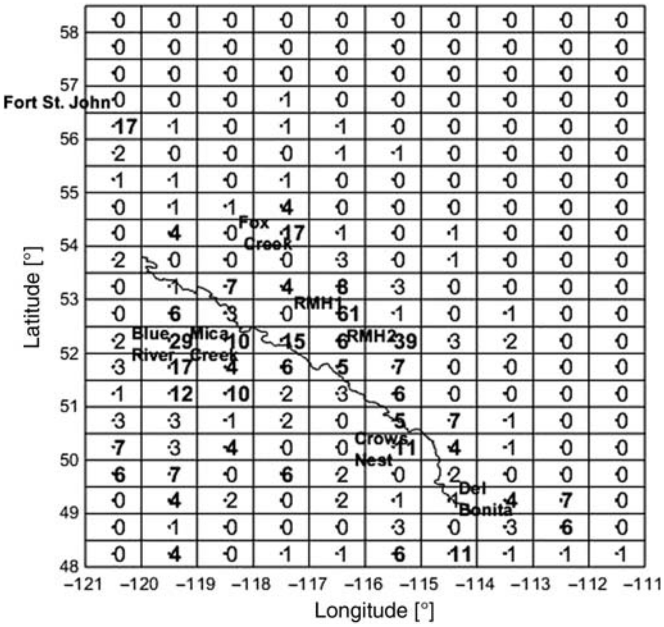

▲ **Figure 8.** Number of earthquakes in the CASC of **M** ≥ M_c from 1985 through 2013 in each grid cell (black points are node centers). Eight cells are named by location. RMH stands for Rocky Mountain House.

The detection threshold M_c (x_i, y_i, Δt) for each node center for each time interval is computed using equations (2) and (3). The numbers plotted in Figure 8 are simple counts of the total number of events that pass the M_c (x_i, y_i, Δt) threshold, from 1985 to 2013, in each grid of the study area. Figure 8 also shows the names of the clusters of seismicity for which there are a significant number of events to examine.

We use a very simple methodology, based on counting, to take a preliminary look at seismicity rates in the eight named clusters shown in Figure 8. To normalize the count to a common basis, as M_c is changing in time and space, we assume that a Gutenberg–Richter relation is applicable, with a nominal b-value of 1.0. The assumed value of b is a typical value for this region, as shown by Adams and Halchuk (2003) and Schultz, Stern, Gu, *et al.* (2015). As a further check on the assumed b-value, we compare the observed rates to that for a Gutenberg–Richter relation with $b = 1.0$, considering a relatively active part of the study region, in a time period of relatively good station coverage. This area, shown in Figure 9, has M_c values that range from 1.7 to 2.3 from 2007 to 2010. It is apparent in Figure 9 that $b \sim 1.0$ for this sample.

We use the number of events above M_c to compute the equivalent count (in each year, for each cell) that should be obtained for **M** ≥ 3, assuming $b = 1$. We refer to this equivalent rate of events as N_{M3}:

$$N_{M3} = N_{M_c(t)} \times 10^{(M_c(t)-3)}, \quad (4)$$

in which M_c (t) references the completeness magnitude during time t, $N_{M_c(t)}$ is the number of events above M_c (t) and N_{M3} is the equivalent number of events above magnitude 3.0.

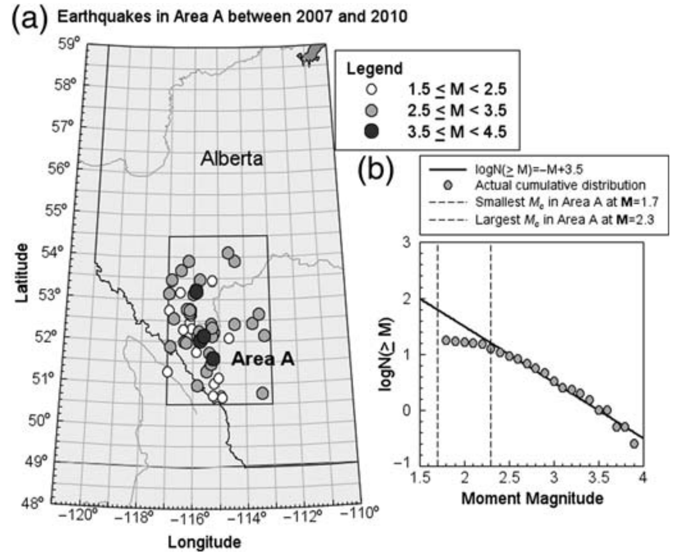

▲ **Figure 9.** Comparison of (a) selected seismicity sample (area A, 2007–2010) with (b) Gutenburg–Richter relation with $b = 1.0$. The dashed lines in (b) represent the range of our M_c estimations for all cells in area A.

Figure 10 shows the equivalent number of **M** ≥ 3 earthquakes per year from 1985 to 2014 for the eight cluster areas, along with corresponding changes of M_c. In most of these clusters, there have clearly been changes in rate over time, with some areas tending to turn on then off. Areas such as Fox Creek have turned on very recently, due to the recent hydraulic fracturing in that area (Schultz, Stern, Novakovic, *et al.*, 2015; Atkinson *et al.*, 2016). Although M_c has been reduced since 2000 for almost all of the eight regions, the occurrence rate of **M** ≥ 3 earthquakes has increased mostly in specific areas near Fox Creek, Blue River1, and Crows Nest. An inspection of the regions having relatively high seismicity rates confirms that there is little correlation between M_c and the occurrence rate of **M** ≥ 3 earthquakes overall. The increased rate of activity in specific areas such as Fox Creek is believed to be related to industry activity (Schultz, Stern, Novakovic, *et al.*, 2015; Atkinson *et al.*, 2016), not to any increase in the number of seismic stations. More detailed investigation of rate changes will be enabled by richer catalogs as additional seismicity continues to be recorded. The results of this study provide the essential information on the magnitude of completeness that is needed to conduct those more detailed investigations.

DATA AND RESOURCES

The Composite Alberta Seismicity Catalog (CASC) is available at http://www.inducedseismicity.ca/catalogues/ (last accessed March 2016) (Fereidoni and Cui, 2015). Information on the stations of the Canadian National Seismograph Network (CNSN) were obtained at http://www.earthquakescanada.nrcan.gc.ca/stndon/CNSN-RNSC/stnbook-cahierstn/index-eng.php (last accessed November 2015). Information on the stations of the TransAlta Dam Monitoring Network (TD) is available from

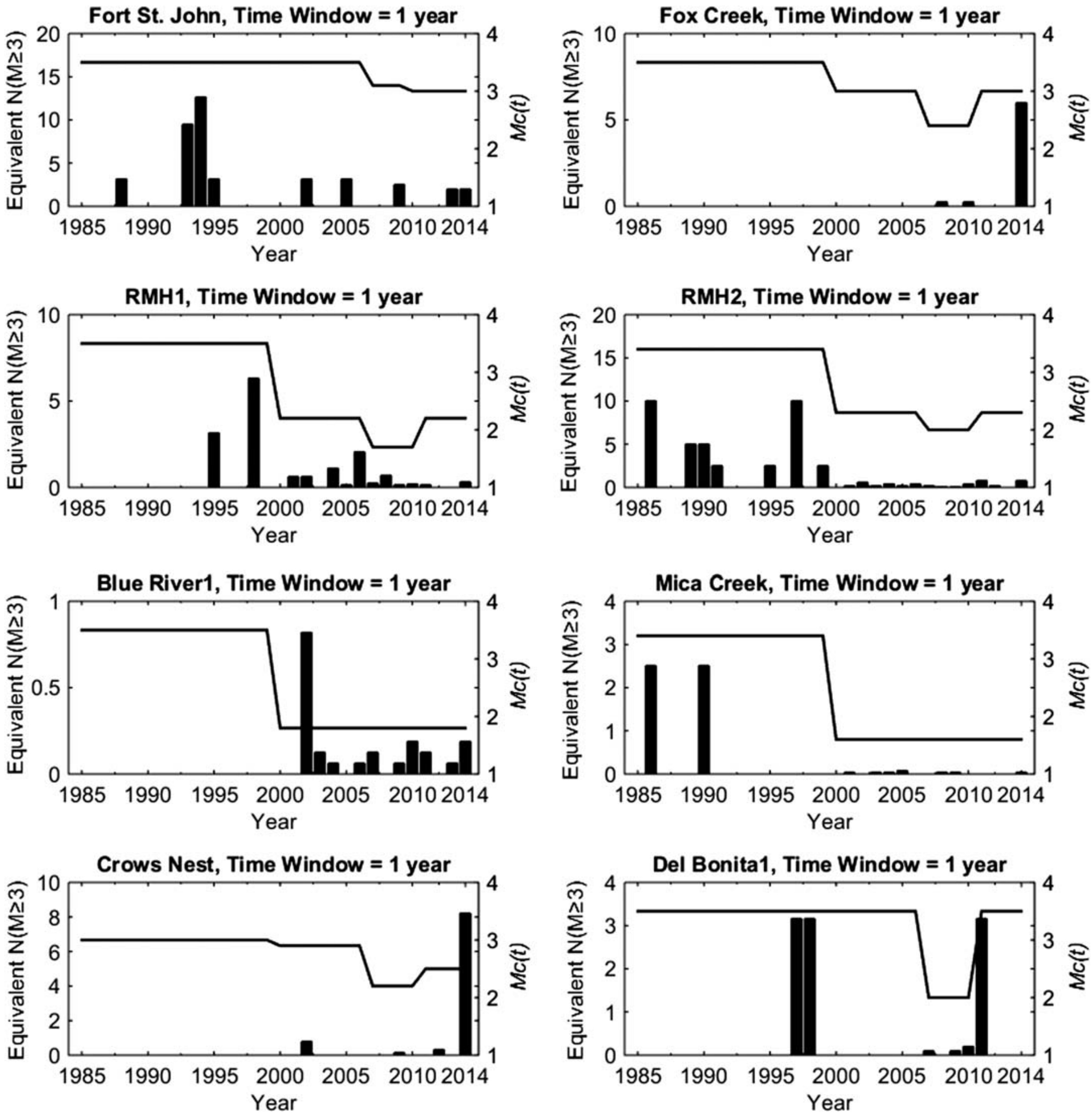

▲ **Figure 10.** Histograms of equivalent number of occurrences of **M** ≥3 earthquakes per year from 1985 to 2014 for eight clusters identified in Figure 8 and corresponding $M_c(t)$. The black bars illustrate the equivalent N(**M** ≥3) calculated from equation (4). The black lines reflect the changes of M_c in each region.

Incorporated Research Institutions for Seismology (IRIS) at http://ds.iris.edu/mda (last accessed November 2015).

ACKNOWLEDGMENTS

This work was funded as part of Natural Sciences and Engineering Research Council of Canada (NSERC)/TransAlta/Nanometrics Industrial Research Chair in Hazards from induced seismicity. We thank two anonymous reviewers and the editor for their constructive comments that led to improvements in the article.

REFERENCES

Adams, J., and S. Halchuk (2004). Fourth-generation seismic hazard maps for the 2005 national building code of Canada, *Proc. of* *the 13th World Conference on Earthquake Engineering*, Vancouver, Canada, 1–6 August 2004, Paper Number 2502.

Atkinson, G., D. Eaton, H. Ghofrani, D. Walker, B. Cheadle, R. Schultz, R. Shcherbakov, K. Tiampo, Y. Gu, R. Harrington, Y. Liu, M. van der Baan, and H. Kao (2016). Hydraulic fracturing and seismicity in the Western Canada Sedimentary Basin, *Seismol. Res. Lett.* **87,** doi: 10.1785/0220150263.

Atkinson, G. M., H. Ghofrani, and K. Assatourians (2015). Impact of induced seismicity on the evaluation of seismic hazard: Some preliminary considerations, *Seismol. Res. Lett.* **86,** no. 3, 1009–1021, doi: 10.1785/0220140204.

Baranova, V., A. Mustaqeem, and S. Bell (1999). A model for induced seismicity caused by hydrocarbon production in the Western Canada Sedimentary Basin, *Can. J. Earth Sci.* **36,** no. 1, 47–64.

Natural Resources Canada (NRCan) (2015). *CNSN Station Book Index*, Retrieved 30 June 2015, http://www.earthquakescanada.nrcan.gc.ca/stndon/CNSN-RNSC/stnbook-cahierstn/index-eng.php (last accessed December 2015).

BC Oil and Gas Commission (2012). Investigation of observed seismicity in the Horn River Basin, 29 pp, http://www.bcogc.ca/document.aspx?documentID=1270 (last accessed December 2015).

Eaton, D. W., and A. B. Mahani (2015). Focal mechanisms of some inferred induced earthquakes in Alberta, Canada, *Seismol. Res. Lett.* **86,** no. 4, doi: 10.1785/0220150066.

Farahbod, A. M., H. Kao, D. M. Walker, J. F. Cassidy, and A. Calvert (2015). Investigation of regional seismicity before and after hydraulic fracturing in the Horn River basin, northeast British Columbia, *Can. J. Earth Sci.* **52,** no. 2, 112–122.

Fereidoni, A., and L. Cui (2015). *Composite Alberta Seismicity Catalog: CASC2014-x*, http://www.inducedseismicity.ca/wp-content/uploads/2015/01/Composite-Alberta-Seismicity-Catalog3.pdf (last accessed March 2016).

Gutenberg, B., and C. F. Richter (1944). Frequency of earthquakes in California, *Bull. Seismol. Soc. Am.* **34,** no. 4, 185–188.

Horner, R. B., J. Barclay, and J. MacRae (1994). Earthquakes and hydrocarbon production in the Fort St. John area of northeastern British Columbia, *Can. J. Explor. Geophys.* **30,** no. 1, 39–50.

Mignan, A., and J. Woessner (2012). Estimating the magnitude of completeness for earthquake catalogs, *Community Online Resource for Statistical Seismicity Analysis*, doi: 10.5078/corssa-00180805.

Mignan, A., M. Werner, S. Wiemer, C.-C. Chen, and Y.-M. Wu (2011). Bayesian estimation of the spatially varying completeness magnitude of earthquake catalogs, *Bull. Seismol. Soc. Am.* **101,** no. 3, 1371–1385.

Milne, W. G. (1970). The Snipe Lake, Alberta earthquake of March 8, 1970, *Can. J. Earth Sci.* **7,** no. 6, 1564–1567, doi: 10.1139/e70-148.

Milne, W. G., G. C. Rogers, R. P. Riddihough, G. A. McMechan, and R. D. Hyndman (1978). Seismicity of western Canada, *Can. J. Earth Sci.* **15,** no. 7, 1170–1193, doi: 10.1139/e78-123.

Plenkers, K., D. Schorlemmer, and G. Kwiatek (2011). On the probability of detecting picoseismicity, *Bull. Seismol. Soc. Am.* **101,** no. 6, 2579–2591.

Rydelek, P. A., and I. S. Sacks (1989). Testing the completeness of earthquake catalogues and the hypothesis of self-similarity, *Nature* **337,** no. 6204, 251–253.

Schorlemmer, D., and J. Woessner (2008). Probability of detecting an earthquake, *Bull. Seismol. Soc. Am.* **98,** no. 5, 2103–2117.

Schorlemmer, D., F. Mele, and W. Marzocchi (2010). A completeness analysis of the National Seismic Network of Italy, *J. Geophys. Res.* **115,** no. B04308, doi: 10.1029/2008JB006097.

Schultz, R., V. Stern, and Y. J. Gu (2014). An investigation of seismicity clustered near the Cordel Field, west central Alberta, and its relation to a nearby disposal well, *J. Geophys. Res.* **119,** no. 4, 3410–3423.

Schultz, R., V. Stern, Y. J. Gu, and D. Eaton (2015). Detection threshold and location resolution of the Alberta Geological Survey earthquake catalogue, *Seismol. Res. Lett.* **86,** no. 2A, doi: 10.1785/0220140203.

Schultz, R., V. Stern, M. Novakovic, G. Atkinson, and Y. J. Gu (2015). Hydraulic fracturing and the Crooked Lake Sequences: Insights gleaned from regional seismic networks, *Geophys. Res. Lett.* **42,** no. 8, 2750–2758, doi: 10.1002/2015GL063455.

Stern, V. H., R. J. Schultz, L. Shen, Y. J. Gu, and D. W. Eaton (2013). *Alberta Earthquake Catalogue*, Version 1.0: September 2006 through December 2010, Alberta Energy Regulator, 29 pp.

Wiemer, S., and M. Wyss (2000). Minimum magnitude of completeness in earthquake catalogs: Examples from Alaska, the Western United States, and Japan, *Bull. Seismol. Soc. Am.* **90,** no. 4, 859–869, doi: 10.1785/0119990114.

Woessner, J., and S. Wiemer (2005). Assessing the quality of earthquake catalogues: Estimating the magnitude of completeness and its uncertainty, *Bull. Seismol. Soc. Am.* **95,** no. 2, 684–698.

Luqi Cui
Gail M. Atkinson
Department of Earth Sciences
Western University
London, Ontario
Canada N6A 5B7
gmatkinson@aol.com

Published Online 15 June 2016